Soft Matter

Quantifying vorticity in magnetic particle suspensions driven by symmetric and asymmetric multiaxial fields

Journal:	*Soft Matter*
Manuscript ID:	SM-ART-04-2015-000966.R2
Article Type:	Paper
Date Submitted by the Author:	31-Jul-2015
Complete List of Authors:	Martin, James; Sandia National Laboratories, Nanomaterials Sciences Solis, Kyle; Sandia National Laboratories, Nanomaterials Sciences

Soft Matter

ARTICLE

Quantifying vorticity in magnetic particle suspensions driven by symmetric and asymmetric multiaxial fields

Received 00th January 20xx,
Accepted 00th January 20xx

DOI: 10.1039/x0xx00000x

www.rsc.org/

J. E. Martin,[a] and K. J. Solis[a]

We recently reported two methods of inducing vigorous fluid vorticity in magnetic particle suspensions. The first method employs *symmetry-breaking rational fields*. These fields are comprised of *two* orthogonal ac components whose frequencies form a rational number and an orthogonal dc field that breaks the symmetry of the biaxial ac field to create the parity required to induce deterministic vorticity. The second method is based on *rational triads,* which are fields comprised of *three* orthogonal ac components whose frequency ratios are rational (*e.g.,* 1:2:3). For each method a symmetry theory has been developed that enables the prediction of the direction and sign of vorticity as functions of the field frequencies and phases. However, this theory has its limitations. It only applies to those particular phase angles that give rise to fields whose Lissajous plots, or principal 2-d projections thereof, have a high degree of symmetry. Nor can symmetry theory provide a measure of the magnitude of the torque density induced by the field. In this paper a functional of the multiaxial magnetic field is proposed that not only is consistent with all of the predictions of the symmetry theories, but also quantifies the torque density. This functional can be applied to fields whose Lissajous plots lack symmetry and can thus be used to predict a variety of effects and trends that cannot be predicted from the symmetry theories. These trends include the dependence of the magnitude of the torque density on the various frequency ratios, the unexpected reversal of flow with increasing dc field amplitude for certain symmetry-breaking fields, and the existence of off-axis vorticity for rational triads, such as 1:3:5, that do not have the symmetry required to analyze by symmetry theory. Experimental data are given that show the degree to which this functional is successful in predicting observed trends.

1 Introduction

Methods of inducing vigorous noncontact fluid flow are important to technologies involving heat and mass transfer and fluid mixing, since they eliminate the need for moving parts, pipes and seals, all of which compromise reliability. Unfortunately, noncontact methods of inducing strong organized flows are few, and have limitations of their own. For example, natural convection [1–3] requires both gravity and a destabilizing thermal gradient. Magnetohydrodynamics [1] requires the injection of large currents into conducting liquids and high magnetic fields. Thermomagnetic convection in ferrofluids [4,5] requires gravity, a destabilizing thermal gradient and a large magnetic field gradient, which makes scaling to large volumes challenging. A more flexible method that eliminated these requirements would be amenable to a broad range of applications.

We have discovered several classes of triaxial fields of modest strength that induce vigorous noncontact fluid flow in dilute magnetic particle dispersions without requiring gravity, a thermal gradient, or a magnetic field gradient. Such fields can create flow lattices [6], vortex lattices and vortex fluids [7, 8]. These induced flows have been used to direct droplet motion [9], create a thermal valve [10], effect active, directed wetting [7], and stimulate a variety of biomimetic dynamics [9]. However, at this point our understanding of these flows is based only on the symmetry of the multiaxial fields and this non-quantitative approach is useful only for certain highly symmetric fields. In this study a functional of the magnetic field is introduced that pertains to the measurable fluid torque densities. The purpose of this study is to investigate the degree to which this functional conforms to the wide range of observed phenomena, to demonstrate that it conforms to the many predictions of symmetry theory, and to use this functional to make predictions where symmetry theory cannot be applied.

1.1 Symmetry theory background

The symmetry theories we have developed are for two classes of fields that induce vorticity, each of which is comprised of three orthogonal components. The first class we call *symmetry-breaking rational fields* [7,8]. These fields employ two alternating components and one dc component. The frequencies of the ac components form a rational number *l*:*m*, where *l* and *m* are relative primes, so either one or both are odd. The second class of fields we call *rational triads* [11], which differ in that all three components are alternating. Once again the frequency ratios are rational numbers, such as 1:2:3.

[a] *Address here.*
[b] *Address here.*
[c] *Address here.*
† Footnotes relating to the title and/or authors should appear here. Electronic Supplementary Information (ESI) available: [details of any supplementary information available should be included here]. See DOI: 10.1039/x0xx00000x

For both field classes it can be shown that the dynamic fields have the symmetry of vorticity and thus have the parity required to allow deterministic fluid vorticity and flow reversal.

The primary goal of the symmetry theories is to predict whether deterministic vorticity can occur and if so, to predict the direction of the fluid vorticity vector and the field changes required to reverse the sign of the vorticity without changing its magnitude. For symmetry-breaking rational fields the predictions are that the vorticity axis is parallel to the odd axis unless both axes are odd, in which case it is parallel to the dc field. Only if the vorticity is around an ac axis does reversing the dc field reverse the flow, but changing the phase of the high frequency (*m*) component by 180°/*l* (*l* ≤ *m*) always reverses the flow. These predictions have been experimentally confirmed for all fields investigated [8].

For rational triads the symmetry theory predicts that vorticity occurs around the field component whose reduced frequency has unique numerical parity (*e.g.*, the "2" in 1:2:3). In the case where all reduced frequencies are odd (*e.g.*, 1:3:5) the dynamic field does not have the symmetry of vorticity, so it is not possible to make predictions about flow with this approach. Symmetry theory also predicts the phase changes required to reverse flow at constant magnitude. These predictions have also been experimentally confirmed for the fields we have investigated [11].

Symmetry theory has some limitations. First, it is not possible to make predictions for fields whose Lissajous trajectories are not highly symmetrical. For symmetry-breaking fields these 2-d trajectories occur at particular phase angles between the two ac components. For example, for a 1:2 field these special phase angles (applied to the high frequency component) are 0°, 90°, 180°,… In all cases there are four distinct Lissajous trajectories that can be treated out of this 1-d set of continuous phases. All other phase angles cannot be treated. For rational triads the symmetric Lissajous trajectories can be obtained by applying the phase angles 0°, 90°,180°,… to each of the three frequencies in any combination. It turns out that this creates only 16 distinct 3-d Lissajous trajectories that can be analyzed out of the 2-d set of independent phase angles (there are only two independent phases for three frequencies since the zero of time is unimportant).

A second limitation of symmetry theory is the inability to make any kind of estimate of the *magnitude* of the torque density created within a magnetic particle dispersion subjected to a multiaxial field. Intuitively it is reasonable that a 1:2 symmetry-breaking field will create greater vorticity than a 13:20 field, but there is currently no method of justifying this belief. Even more disconcerting is the inability to deal with the effect of small frequency changes. For example, the symmetry-breaking field 150:100 factors to 3:2, so vorticity is predicted to occur around the high-frequency field axis. But if the low frequency is increased to obtain 150:101 the low frequency axis becomes odd so vorticity should now occur around this axis. But 150:101 can be viewed as a phase-modulated 3:2 field, so we expect to observe oscillating vorticity around the high frequency axis, which is indeed the experimental observation. Symmetry theory cannot address this oscillating flow.

Finally, symmetry theory cannot address the utter peculiarity of the origin of these flows. There is just something strange about predicting vorticity for fields that in general are non-circulating. Yet these flows can be quite vigorous. In fact, the symmetry theory only shows that these flows are allowed and cannot make any statement about whether they should or should not occur. For these reasons it is desirable to have a physically reasonable method that for any given field can produce a torque density vector that produces vorticity. One approach is to simulate the system microscopically. This would lead to an understanding of the microscopic magnetic particle dynamics as well as addressing the issues raised above, but such an approach would be extremely time consuming. A second approach is to develop a closed-form theory of the microscopic particle dynamics that can at least be numerically integrated. A third approach is to use physical insight and previous results to develop a functional that produces the torque vector: This is the approach we have taken as a first step on the path to quantifying vorticity in any multiaxial field.

1.2 Torque density functional

A physically meaningful functional must conform to all of the above-mentioned predictions of the symmetry theories and yet must also conform to various experimental observations. These observations include the finding that the torque density in a particle suspension exposed to a particular field is independent of particle size, liquid viscosity, and the magnitude of the field frequencies, provided that the *Mason* number is below a critical value that permits particle chaining. For the restricted case of a "vortex field," which consists of a rotating field to which an orthogonal dc field is applied, an expression has been derived for the suspension torque density that is based on the analysis of *volatile* particle chains that lag in phase behind the field [12]. This is a phase lag problem in three dimensions for particle chains whose size is determined by various instabilities that lead to fragmentation. This theory successfully accounts for all of the experimental observations on vortex fields, the result being

$$\mathrm{T} = \frac{1}{12}\varphi_p \mu_0 M^2 \sqrt{\sin^2\theta_f - \cos^2\theta_f} \text{ for } \theta_f \geq 45° \qquad (1)$$

where φ_p is the particle volume fraction, μ_0 is the vacuum permeability, *M* is the particle magnetization, and θ_f is the angle the field vector makes to the dc field. For this case the Mason number is defined as $Mn = 9\eta\omega/(2\mu_0 M^2)$, where ω is the field frequency. Eq. 1 is valid when this Mason number is less than ~0.02 for *balanced* vortex fields, those having equal rms field components ($\tan\theta_f = \sqrt{2}$). In the case of linear magnetic polarization the particle magnetization for a dilute suspension is given by $\chi_p H_0$ where $\chi_p = 3$ is the intrinsic susceptibility of a magnetic sphere comprised of a material whose relative permeability greatly exceeds that of the liquid, which is the typical case for soft ferromagnetic particles. In short, the specific torque density T/φ_p is simply proportional to the energy density $\mu_0 H_0^2$ of the field.

The vortex field is a very simple case because it admits a steady-state solution. For other multiaxial fields, such as 1:2:dc the field magnitude is not constant and the axis about which instantaneous field rotation occurs is not so easily described. If we make the approximation that the instantaneous field energy density gives the instantaneous torque density then all that remains is dealing with the direction of the instantaneous torque vector. As a second approximation this torque direction

is taken to be the direction about which the instantaneous field rotates, $\mathbf{H}_0(t)\times\dot{\mathbf{H}}_0(t)\big/\left|\mathbf{H}_0(t)\times\dot{\mathbf{H}}_0(t)\right|$, in other words this vector is normal to the instantaneous rotation plane of the field. If the torque is indeed caused by particle chains lagging the field, then this is a good approximation when the phase lag is small. The torque density functional $\mathbf{J}_{\{\phi\}}$ is thus

$$\mathbf{J}_{\{\phi\}}=\int_0^1\mathbf{J}_{\{\phi\}}(s)\,ds \text{ where } \mathbf{J}_{\{\phi\}}(s)=\left|\mathbf{h}(s)\right|^2\frac{\mathbf{h}(s)\times\dot{\mathbf{h}}(s)}{\left|\mathbf{h}(s)\times\dot{\mathbf{h}}(s)\right|}. \quad (2)$$

where we have indicated explicitly the dependence on the phase angles of the field. Here $s = ft$ is the reduced time, f is a frequency, and **h** is the reduced field. For symmetry breaking fields the reduced field is

$$\mathbf{h}(t)=\frac{\mathbf{H}_0(t)}{H_0}=\sin(l\times 2\pi ft+\phi_l)\hat{\mathbf{x}}+\sin(m\times 2\pi ft+\phi_m)\hat{\mathbf{y}}+\frac{c}{\sqrt{2}}\hat{\mathbf{z}} \quad (3)$$

l and m are relative primes and by convention $l \le m$. The rms reduced field is $\sqrt{2+c^2}\big/\sqrt{2}$. (For a balanced field, where all rms field components are equal $c = 1$.) For the rational triads we restrict our attention to such balanced fields, so

$$\mathbf{h}(t)=\sin(l\times 2\pi ft+\varphi_l)\hat{\mathbf{x}}+\sin(m\times 2\pi ft+\varphi_m)\hat{\mathbf{y}}+\sin(n\times 2\pi ft+\varphi_n)\hat{\mathbf{z}} \quad (4)$$

In this case the rms reduced field is $\sqrt{3/2}$ and to be definite $l \le m \le n$. The predicted torque density is related to the dimensionless torque density functional by $\mathbf{T}=const\times\varphi_p\mu_0H_0^2\mathbf{J}_{\{\phi\}}$.

This expression may be viewed as an *ansatz*, not a theory *per se,* however it produces many useful results that are in accord with experiment and also can be used to successfully predict unexpected effects that we have observed in experiment. Some of these predictions were sufficiently strange that we literally ran down to the lab to verify them, and verify them we did, as will be discussed below.

2 Experimental

The magnetic particle suspension consisted of molybdenum-Permalloy platelets ~50 μm across by 0.4 μm thick (Novamet Corp.) dispersed into isopropyl alcohol at a low volume fraction. The uniform triaxial ac magnetic fields were produced by three orthogonally-nested Helmholtz coils, operating in series resonance with appropriately-configured capacitor banks, two of which employ a computer-controlled fractal design [13]. For the 1:3:5 rational triad field studied in this work the fundamental frequency was 50 Hz and all three induction field components were 150 Grms. The three field components were phase-locked *via* two Agilent/HP function generators (equipped with Option 005), allowing for *stable* control of the phase angle of each component. (If the field components are not phase-locked there will be a very slow phase modulation between the components due to the finite difference in the oscillator frequency of each function generator, preventing meaningful studies of the phase angle.)

To quantify the magnitude of the vorticity, the torque density of the suspension was computed from measured angular displacements on a custom-built torsion balance that is described and pictured in Fig. 2 of reference 7. In this case the suspension (1.5 vol%) was contained in a small vial (1.8 mL) attached at the end of the torsion balance and suspended into the central cavity of the Helmholtz coils *via* a 96.0 cm-long, 0.75 mm-diameter nylon fiber with a torsion constant of ~13 μN·m rad^{-1}.

3 Results and Discussion

3.1 Computations for symmetry-breaking fields

The first issue that must be addressed is whether the functional conforms to the predictions of symmetry theory. The case of a 2:3:dc field with both phase angles set to zero is given in Fig. 1. Recall that vorticity must occur around the high frequency (y) axis in this case. In these figures the three components of the integrand of **J**(s) and its integral are given as functions of the reduced time. This integral corresponds to the rotation of a body subject to this time-dependent torque density. Along both the x and z axes the integrands are perfectly symmetric around zero, so the integral over one cycle is zero and the average slope of the integral, which is proportional to the average torque density, is thus zero. Along the y axis the integral is asymmetric, and the integral has a finite average slope and torque density. So this particular case conforms to the predictions of symmetry theory. In fact, even

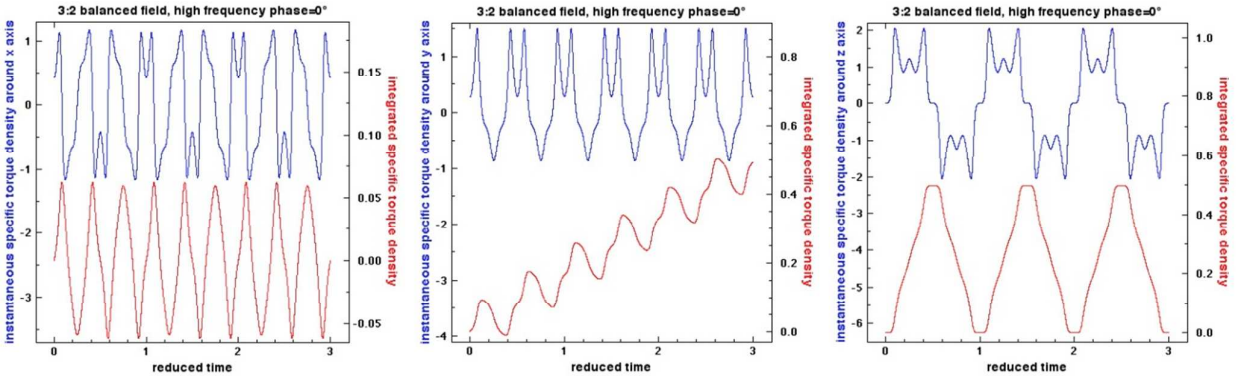

Fig. 1 Instantaneous values of the computed torque functional are given for a 2:3:dc symmetry-breaking field. The integral of these functions corresponds to the rotation of a free body subjected to this torque. A persistent rotation only occurs around the y axis, which is indeed the prediction of symmetry theory. The time-averaged torque density functional is the slope of the integral. It is this slope that pertains to measurement, since the field frequencies are typically in the audio range, generally above 48 Hz in our laboratory and frequently much higher, and so the fluctuations only give rise to rapid fluctuations of the needle in our torsion fiber apparatus.

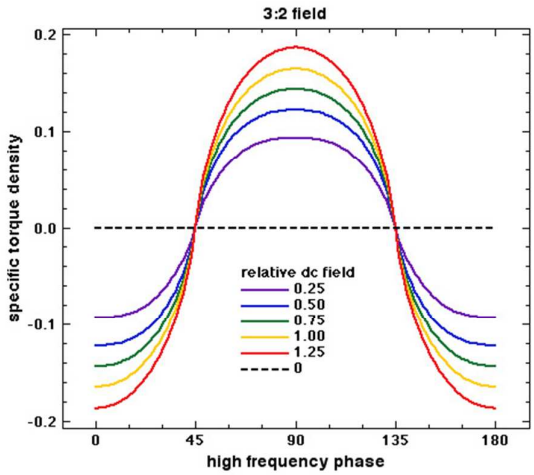

Fig. 2 Computed torque density as a function of the high frequency phase for the 2:3:dc field. The dc field is relative to the rms amplitude of either of the ac field components.

the predicted fluctuations in the torque can be observed experimentally as a jittery torque signal.

3.2 Dependence on phase and dc field

The computed torque density has a strong dependence on the relative phase between the ac field components, as well as on the magnitude of the dc field. This dependence is shown in Fig. 2 for the *y* axis torque created by the 2:3:dc field. At zero dc field the torque functional is zero, in accordance with symmetry theory for even, odd fields, but for finite dc fields the torque is non-vanishing, is periodic on the interval 180°, and can be reversed at constant magnitude by any 90° shift of the high frequency phase, in agreement with both symmetry theory [7] and experiment [8]. Moreover, symmetry theory shows that reversing the dc field reverses the torque for even, odd fields and the torque functional also shows this reversal. In general, for the field *l*:*m* symmetry theory shows that when plotted against the high-frequency phase the torque curve is periodic on the interval 360°/*l* and reverses at constant magnitude for phase shifts of 180°/*l*.

Odd:odd fields differ in that vorticity is symmetry allowed even in the absence of the dc field component and therefore must not reverse upon dc field reversal. Computations for the 1:3 field do indeed show that the torque functional does not vanish in the absence of a dc field, but grows stronger as the dc field increases and cannot be reversed by reversing the dc field. This suggests the possibility of torque when the dc field is replaced by an ac field, a subject discussed below. However, the experimental situation is complicated by the fact that in the absence of the dc component the particles experience a time-averaged interaction that can be described as a negative dipolar interaction, causing the particles to form into parallel stationary sheets [14–17] (like baklava), instead of forming the volatile chains that give rise to vorticity. Because of this competing effect, fluid vorticity *does* require the presence of the dc component, at least for spherical particles. For platelets made of soft ferromagnetic materials the situation is more complex: Although stationary sheets can form in a biaxial field under some circumstances (*e.g.*, very high frequency, very high viscosity, low field), flow instabilities typically occur in the form of a square lattice of antiparallel flow columns normal to the plane of the field [6]. When these columns form in an odd:odd field there is pronounced vorticity as well, the axis of which is parallel to the flow columns. At higher platelet loadings a normal-field instability can occur that causes the particle dispersion to rise up as a ridge, within which a lattice of flow columns can be observed [see Fig. 4 in Reference 6]. The vorticity in the absence of a dc field can be easily confirmed by detuning one of the field components to create a phase modulation that periodically reverses the vorticity. The ridge then sloshes back-and-forth in response to the oscillating vorticity, which brings us to the next issue: field heterodyning.

3.3 Heterodyning

A more interesting problem is that of heterodyning, which occurs when one of the frequencies is detuned to create a modulation of phase and flow reversal. In Fig. 3 are presented

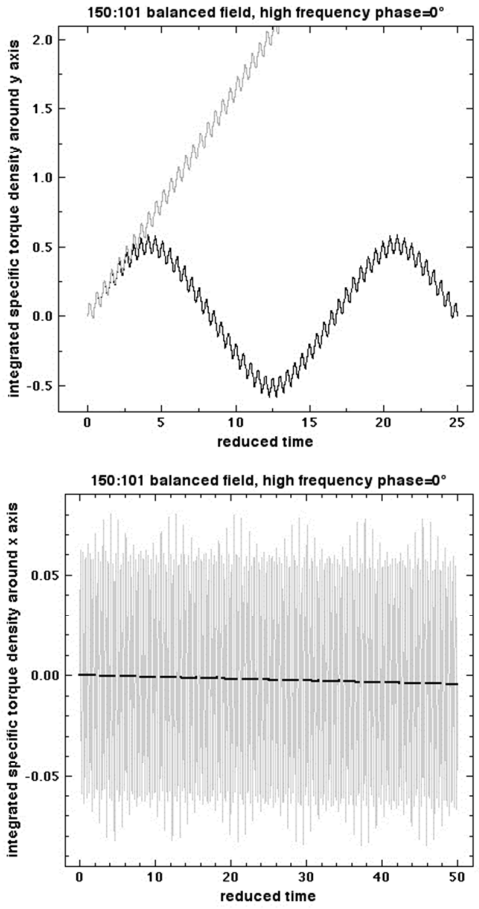

Fig. 3 When a 2:3:dc field is detuned field to 101:150:dc the heterodyne beating creates periodic flow reversal around the *y* axis, which is indeed observed in the laboratory. (top) The torque functional demonstrates this flow reversal and shows that the peak torque density is expected to be the same as for the non-heterodyned field. However, symmetry theory shows that for the 101:150:dc field the average torque can be non-vanishing only around the *x* axis. For this field the torque functional shows that around the *y* axis does indeed average to zero and a small but finite net torque does occur around the *x* axis, as shown at bottom.

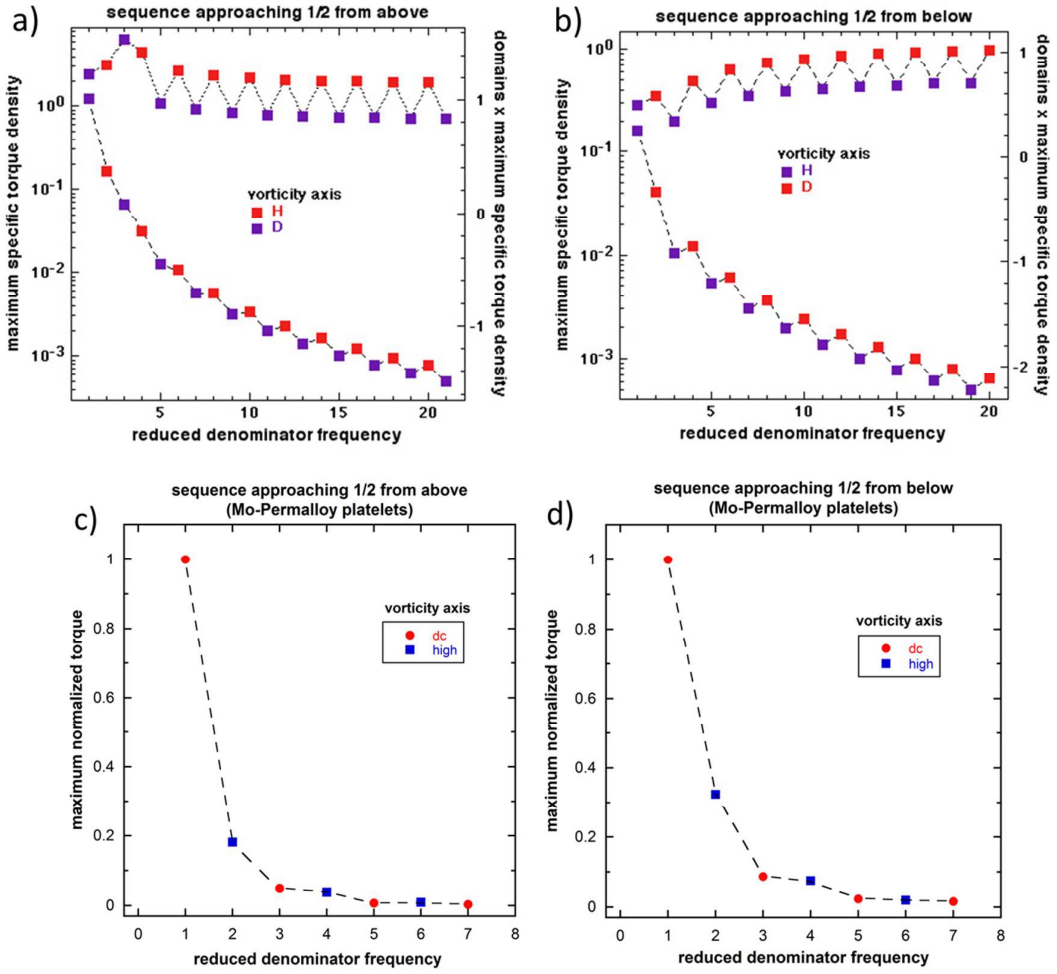

Fig. 4 The maximum of the torque functional as a function of phase is plotted versus the relative denominator frequency for rational number sequences approaching ½ from above and below. Multiplying these peak torques by the number of domains in the 2-d Lissajous plots shows an approach to an asymptote, indicating an algebraic decay. The alternation in the torque axes are predicted by symmetry theory as well. (bottom) Experimental torque data for rational number sequences approaching ½ from above and below show the alternation of the vorticity axis between the high frequency and dc field axes, although the relative magnitude of the torque around each axis is reversed from the trend predicted by the functional. In both cases the magnitude of the torque is observed to decay rapidly as the number of Lissajous domains increases.

computations for the case 101:150:dc. Because this is a modulation of 2:3:dc it is expected that a periodic torque around the *y* axis will occur, and this is indeed observed in the component $J_y(s)$. More importantly, the time-average of this torque is zero, in conformity to symmetry theory. However, symmetry theory allows a finite time-average torque around the *x* axis, and although this torque is quite small, the slope can be seen in the data in Fig. 3(b).

3.4 Torque density for fields of increasing complexity

As the irreducible ratio of the field frequencies requires larger integers to represent, both experiment and intuition indicate that the suspension torque density diminishes, though symmetry theory is uninformative on this point. To examine this issue we have considered a few particular sequences of irreducible rational numbers. The first two sequences arise in investigations of the fractional quantum Hall effect [18] and serve as useful examples here as well. Both of these sequences approach 1/2, one from above [$k/(2k-1)$, $k = 1,2,\ldots$] and one from below [$k/(2k+1)$, $k = 1,2,\ldots$]. All of these calculations are for balanced fields and the phase angle between the field components (either ϕ_x or ϕ_y will do) is varied to find the maximum of the torque functional.

The dependence of $|\mathbf{J}|$ on the denominator of these ratios is shown in Figs. 4(a) and (b). For the sequence approaching ½ from above the torque vacillates between the high frequency and dc field directions, in agreement with symmetry theory, and falls off asymptotically as the inverse of the number of domains *N* in the relevant Lissajous curve, given by $N = lm + (l-1)(m-1)$. Fields such as 21:41 therefore give rise to very small torques in comparison to something like 2:3. For the sequence approaching ½ from below, Fig. 4(b), the behavior is similar, with the odd:odd fields showing somewhat greater torque.

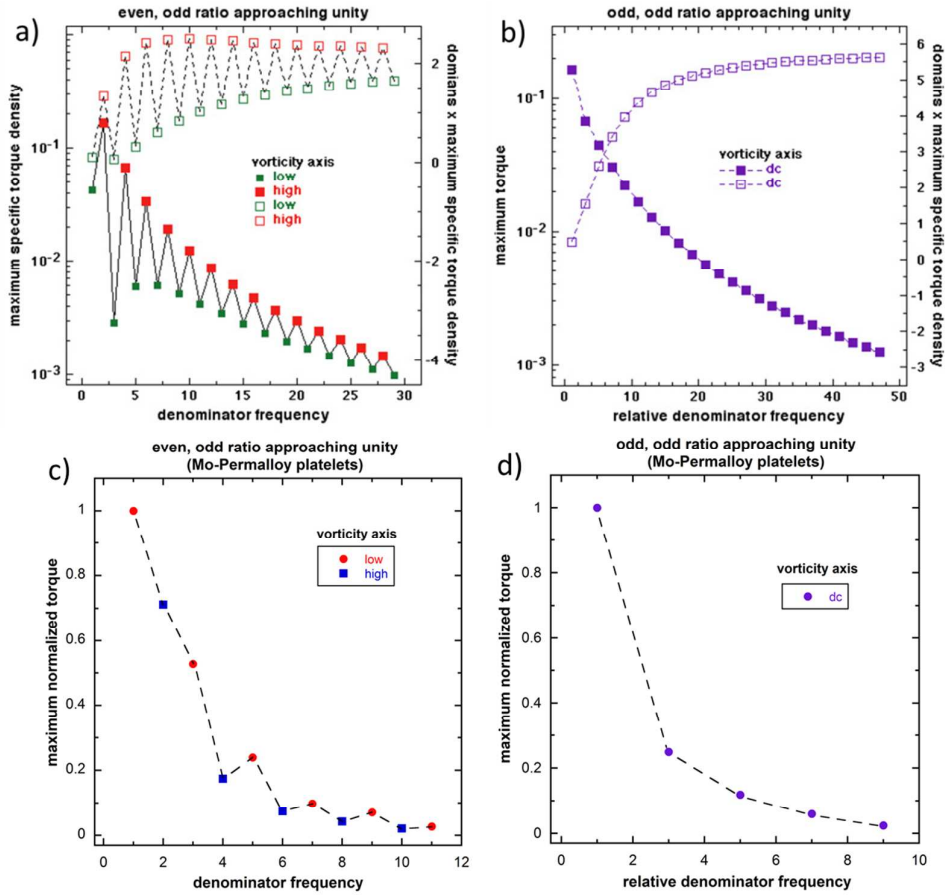

Fig. 5 The maximum of the torque functional as a function of phase is plotted versus the relative denominator frequency for even:odd and odd:odd frequencies approaching unity. Multiplying these peak torques by the number of domains in the 2-d Lissajous plots shows an approach to an asymptote, indicating an algebraic decay. The odd:odd torques are expected to be especially strong. (bottom) Experimental torque data for even, odd ratio approaching unity. An oscillatory series of torques are produced whose vorticity axis alternates between the high and low frequency components. The magnitude of the torque is observed to decay rapidly as the number of Lissajous domains increases.

Both of these sequences were investigated experimentally, with the torque data shown in Figs. 4(c) and (d). The experimental torque values display the alternation of the vorticity axis between the high frequency and dc field axes, in accord with the torque functional and symmetry theory. Furthermore, an oscillatory trend in the relative magnitudes of the torques between the two vorticity axes is also observed; however, the trend in the relative magnitudes is reversed from that predicted by the functional. The reason for this discrepancy is not clear. Finally, the overall magnitude of the torque is observed to decay rapidly with increasing denominator frequency, corresponding to an increasing number of Lissajous domains.

Two sequences approaching unity were investigated as well. The first consists of irreducible ratios containing an even integer, $[k/(k+1),\ k = 1,2,\ldots]$, and the second consists of only odd numbers, $[(2k-1)/(2k+1),\ k = 1,2,\ldots]$. Fig. 5(a) shows that for the even, odd field sequence there is an oscillation between the torque being around the low and high frequency axis, as expected from symmetry theory, and that the maximum torque is again asymptotically scaling as the inverse number of domains in the Lissajous plot. For odd:odd fields the torque is predicted to occur only around the dc field direction and once again it falls off as the inverse number of domains, Fig. 5(b), but the amplitude is much larger for any given domain number than for the other cases investigated.

Experimental torque data were also collected for the even, odd sequence approaching unity, Figs. 5(c) and (d). In accord with the predicted data from the functional in Fig. 5(a), the experimental torque values display an oscillatory behavior as the overall magnitude rapidly decays with increasing denominator frequency. The oscillations in torque correspond to the vorticity axis alternating between the high and low frequency components. However, as was observed with the sequences approaching ½ from above and below, the trend in the relative magnitudes between the two vorticity axes is reversed from that predicted by the functional. The odd:odd ratio approaching unity was also investigated, Fig. 5(d), in which case the torque only occurs around the dc field axis and falls off rapidly with increasing denominator frequency.

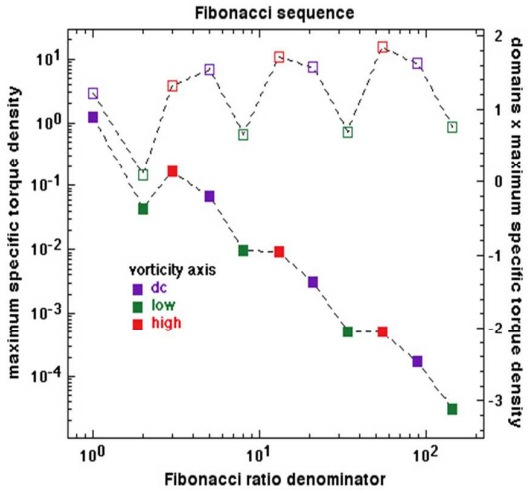

Fig. 6 The Fibonacci sequence creates a periodic transition between all three field axes and once again the peak torque falls off as the inverse of the number of domains.

Finally, neighboring terms in a Fibonacci sequence are relative primes and so make sequences of irreducible rational numbers. We investigated the sequence 1:1, 1:2, 2:3, 3:5, 5:8, 8:13,… This sequence approaches the inverse golden ratio. The maximum torque functional for this sequence is plotted in Fig. 6. The vorticity axis is observed to form the repeated axis sequence dc, low, high, which is once again in accord with symmetry theory. Once again the torque falls off as the inverse number of domains in the Lissajous plots.

3.5 Flow reversal

In a previous publication [8] we reported a very strange observation for a 1:2 field. After applying the ac fields the dc field was slowly ramped up, which caused fluid vorticity to initiate and progressively increase. As the field was progressively increased further the vorticity slowed down, stopped, and then reversed direction. Symmetry theory cannot address this issue, but can the torque functional shed light on this? In Fig. 7 calculations are shown for a 1:2 field over a range of dc field strengths, ranging from $c = 0$ to 1.25 (see Eq. 3). Flow reversal occurs at roughly $c = 0.75$, which is commensurate with experimental observations of surface flow [8]. We pursued this issue by investigating many different symmetry-breaking fields and for all fields of the form odd:odd + 1 that we have investigated flow reversal is indicated. We can find no other fields where the torque functional indicates flow reversal.

3.6 Inducing vorticity with biaxial fields?

It is quick and easy to investigate a lot of ideas with the torque functional, including ideas that might be difficult to screen experimentally. Symmetry-breaking rational fields consist of three orthogonal components and thus are three-dimensional fields. Is it possible to initiate strong vorticity with fields confined to a plane? Take for example the biaxial field in the *x*-*y* plane with frequency ratio 2:3. Recall that this field produces vorticity around the *y* axis when a dc field is applied along the *z* axis. If instead a dc field is applied along the *y* axis, which is the odd axis, the torque functional indicates torque around the *z* axis, Fig. 8. The dependence of the torque functional on

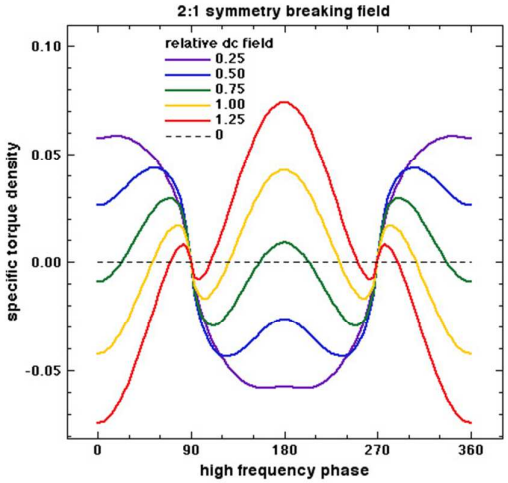

Fig. 7 For all of the odd:odd+1:dc fields we have investigated (1:2, 3:4,…) the torque functional indicates flow reversal with increasing field. Flow reversal seems to be unique to this class of fields.

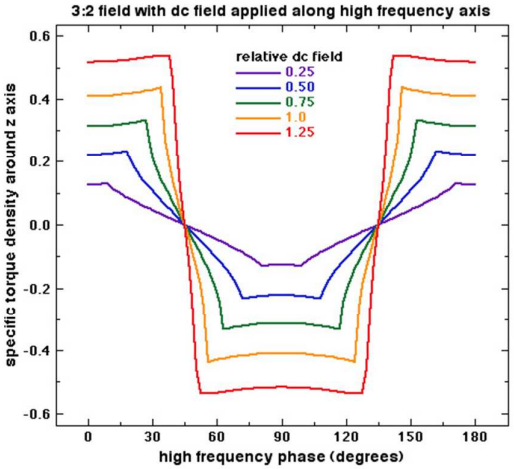

Fig. 8 When a dc field is applied along the high frequency axis of a 2:3 field the resulting biaxial field produces torque around the normal to the field plane.

phase angle approaches a square wave, which is striking. The *z* axis is a C_2 symmetry axis for this case when one considers the equivalency of the field and its converse and the other two axes are antisymmetric under a 180° rotation. Because this symmetry is shared by vorticity around the *z* axis this observation could have been anticipated. Experiments on platelet suspensions do indeed confirm this prediction. On the other hand, if a dc field is applied along the *x* axis the torque functional predicts that vorticity will not occur, and it is notable that all three axes are C_2 axes for the field and its converse, which is not the symmetry of vorticity.

Similar observations apply to the 1:2 field: when a dc field is applied along the odd axis (which in this case is the low frequency axis) the torque functional indicates torque around the *z* axis. When a dc field is applied along the even axis the functional predicts no torque. Again, this behavior could have been anticipated from the symmetry of the trajectories. It would appear that all even, odd fields are capable of producing a *z* axis torque when a dc field is applied along the odd field component.

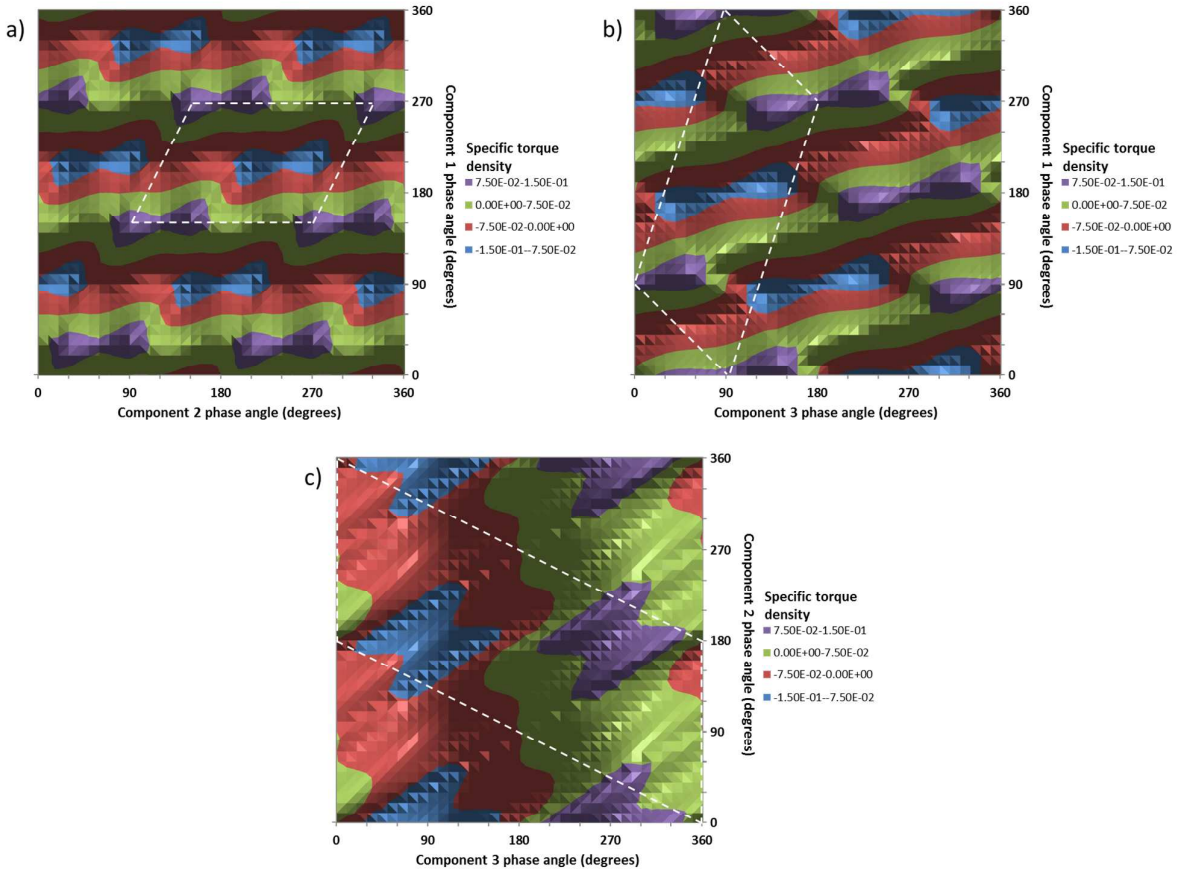

Fig. 9 The torque functional correctly predicts torque around the *y* axis for the 1:2:3 field. Here this torque density is plotted as a function of the three possible sets of phases.

As discussed above, odd:odd fields produce torque around the *z* axis even in the absence of a dc field, because odd:odd fields possess the symmetry of vorticity, with the *z* axis being the C_2 axis of symmetry. Applying a dc field along either of the ac components does not change this symmetry and does not appreciably alter the dependence of the torque functional on phase angle. Odd:odd fields do not seem to be interesting as regards the addition of in-plane dc fields. However, suspensions of spherical particles have a strong tendency to form particle sheets, and the dc field component reduces this tendency, allowing the particles to form the chains that presumably give rise to the torque.

3.7 Rational triads

The experimental investigation of the torque generated by rational triads is time consuming because there are two independent phase angles. If torque measurements are made at 10° intervals for each of the two phase angles over 1200 measurements are required. At roughly 5 minutes per measurement that requires 100 hrs. of continuous work. Any new ideas about rational fields are therefore tough to sort through, especially those that might lead to off-axis vorticity (see below), which could triple the measurement time, since measurements would in general have to be made along all three field directions. In contrast, it is a matter of much less than a minute to compute the torque functional for the same set of phase angles. These results are sufficiently useful to guide experimental work. In the following we will explore the torque density functional for the specific cases of the four classes of rational triads, three of which we have previously investigated experimentally [11].

In previous work we have shown that there are four classes of rational triads [11]. The first is even, odd, odd and 1:2:3 is the simplest example of this class. Symmetry theory shows that this field produces vorticity around the even axis. The second class is even, even, odd fields with even:even factoring to even:odd. A simple example of this class is 2:3:4 and symmetry theory shows that vorticity is around the odd axis for this class (*i.e.*, "3" in this case). The third class is even, even, odd with even:even factoring to odd:odd and once again symmetry theory predicts vorticity around the odd axis. The example of this class that was experimentally investigated in our previous paper is 1:2:6. Finally, the fourth class is odd:odd:odd, for which symmetry theory could not make predictions, simply because fields of this class do not have the symmetry of vorticity. These fields can be treated by the torque density functional, however, which we will find predicts off-axis vorticity for the example field 1:3:5.

The symmetry theory for rational triads is based on those 3-d Lissajous trajectories that have highly symmetric projections on faces normal to each of the three field

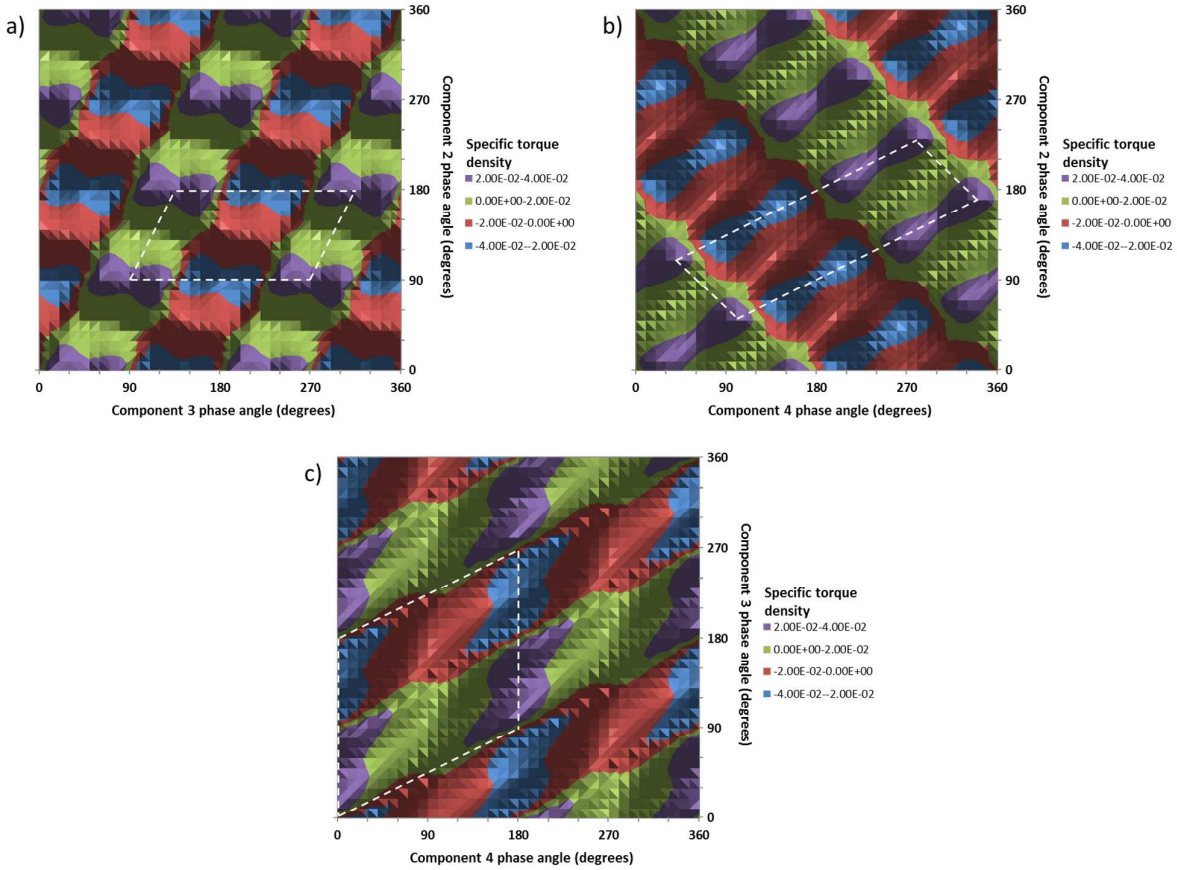

Fig. 10 The torque functional correctly predicts torque around the *y* axis for the 2:3:4 field. The torque density is plotted as a function of the three possible sets of phases.

directions. These symmetric 3-d trajectories can be expressed by assigning to each of the three sine terms in Eq. 4 one of the phases 0°, 90°, 180°, 270°, corresponding to sine, cosine, −sine, −cosine. There are thus 4 × 4 × 4 = 64 symmetric 3-d Lissajous trajectories that can be treated by symmetry theory. These 64 trajectories can be classified into 4 groups of 16. In each of these groups the magnitude of the torque density is fixed, but 8 of the trajectories give clockwise flow and 8 give counterclockwise. In addition to predicting the vorticity axis symmetry theory also predicts these groups and the relative vorticity sign for each trajectory within each group.

The 1:2:3 triad—Calculations for the 1:2:3 field show that vorticity does indeed occur around the even axis. In Fig. 9 calculations are presented for the torque functional as a function of each possible set of two independent phase angles, (ϕ_1, ϕ_2), (ϕ_2, ϕ_3) and (ϕ_1, ϕ_3). Of course, all of these data sets contain the same information and can be related to each other by a change of variables. For the 1:2:3 field the equivalent phase angles are $(\phi_1,\phi_2,0)$, $(\phi_1-\frac{1}{2}\phi_2,0,-\frac{3}{2}\phi_2)$, $(0,\phi_2-2\phi_1,-3\phi_1)$.

In the (ϕ_1, ϕ_2) plane one lattice vector that defines the unit cell (a vector that preserves torque density) is seen from Fig. 9(a) to be **A**=(0°, 180°). Substituting this phase shift into Eq. 4 (with $\phi_3 = 0$) gives

$$\mathbf{h}(t) = \frac{\mathbf{H}_0(t)}{H_0} = -\cos(ls' + \phi_l)\hat{\mathbf{x}} + \sin(ms' + \phi_m)\hat{\mathbf{y}} + \cos(ns')\hat{\mathbf{z}} \quad (5)$$

where $s' = s + 90°$. The torque equivalence of the fields [−C, S, C] {abbreviation for [−cos(1*s*), sin(2*s*), cos(3*s*)]} and [S, S, S], is in accord with symmetry theory, as shown in Table 5 of Reference 11. The second lattice vector is **B** = (120°, 60°). The change of variables $s' = s + 30°$ leads to [C, S, −C], which is also shown by symmetry theory to be equivalent to [S, S, S]. Experimental data need only be taken over this unit cell, which is only 1/6 the computed area. The lattice vectors are those phase changes that preserve vorticity. To reverse vorticity at constant magnitude requires a phase change of (60°, 120°).

It is interesting to examine how the unit cell transforms in other data planes. For the (ϕ_1, ϕ_3) plane the lattice vectors **A** and **B** become (270°, 90°) and (90°, −90°), which is the rather large and experimentally awkward unit cell observed in Fig. 9(b). In the (ϕ_2, ϕ_3) plane the lattice vectors **A** and **B** transform to (180°, 0°) and (−180°, 360°) to create the unit cell apparent in Fig. 9(c). (Of course, a simpler choice for the unit cell is the lower half of the plane.) In any case, the torque functional can determine which pair of phase shifts leads to a unit cell

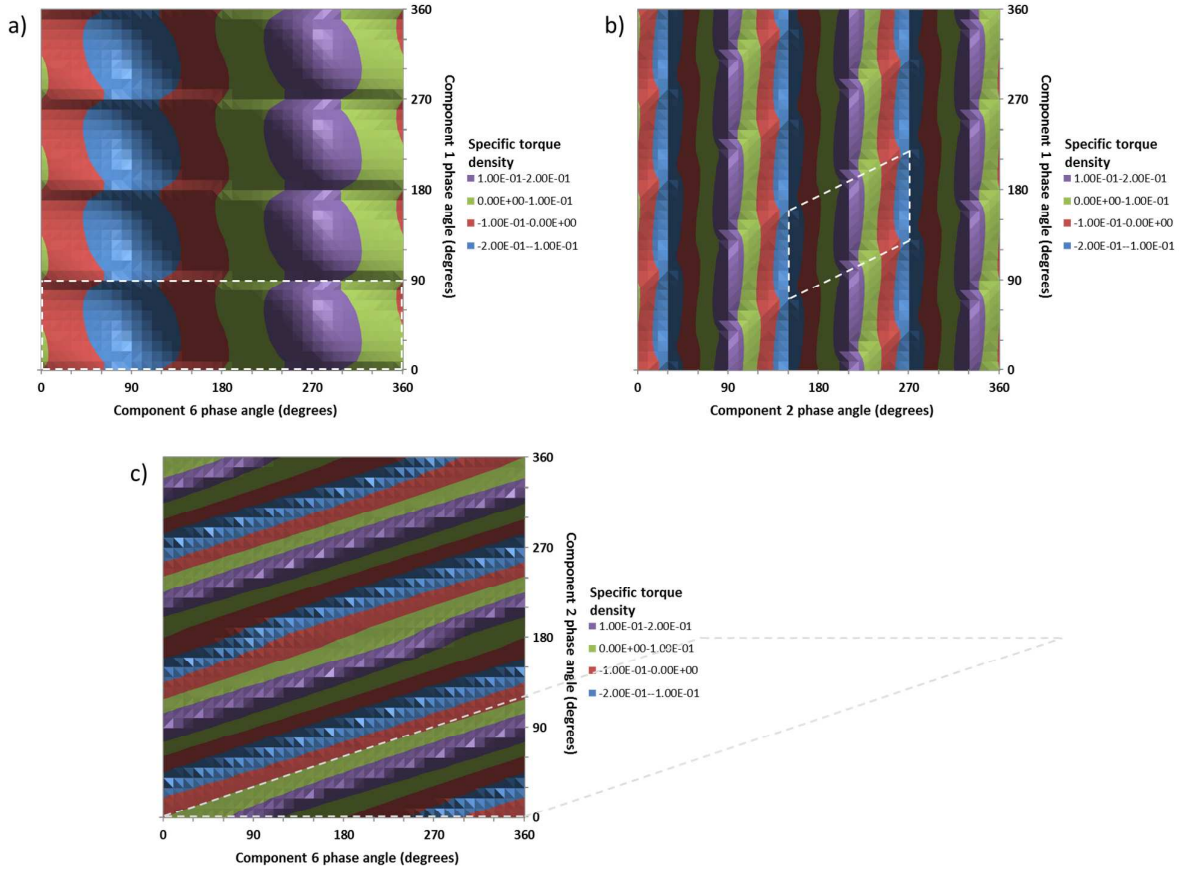

Fig. 11 The torque functional correctly predicts torque around the *x* axis for the 1:2:6 field. Again the torque density is plotted as a function of the three possible sets of phases.

suitable for experimental investigation, and avoids the issue of taking redundant data. In the (ϕ_1, ϕ_3) plane flow reversal at constant magnitude requires a phase shift of (90°, 90°) and in the (ϕ_2, ϕ_3) the required phase shift is (0°, 180°).

The torque functional can also be computed for the exact phases of all of the 64 symmetric 3-d Lissajous trajectories presented in Table 5 of Reference 11. These computations show that within each group of 16 fields the torque magnitude is indeed constant and the computed relative vorticity signs (CW or CCW) are in agreement as well.

Previously reported experimental data were collected in the (ϕ_1, ϕ_3) plane and demonstrate the predicted lattice vectors. However, the "dog bone" shaped peaks and valleys in Fig. 9(a) are merely elongated single peaks in these data.

The 2:3:4 triad—In this case the torque functional shows torque around the odd axis ("3), in accord with the predictions of symmetry theory. The equivalent phase angles are $(\phi_2,\phi_3,0)$, $(\phi_2-\frac{2}{3}\phi_3,0,-\frac{4}{3}\phi_3)$, $(0,\phi_3-\frac{3}{2}\phi_2,-2\phi_2)$ and in the (ϕ_2, ϕ_3) plane lattice vectors are **A**=(0°, 180°) and **B**=(90°, 45°), Fig. 10(a). These phase shifts transform [S, S, S] to [S, −S, S] and [S, −C, −S], respectively. Table 1 of the Electronic Supplementary Information (ESI) for Reference 11 shows that symmetry theory shows the equivalence of [S, S, S], [S, −S, S], and [C, −S, −S]. Moreover, torque functional calculations for the 64 symmetric Lissajous trajectories within this table are in agreement with the vorticity magnitude and sign groupings. Flow reversal at constant magnitude can be achieved by the phase change (0°, 90°).

The lattice vectors **A** and **B** become (120°, 240°) and (60°, −60°) in the (ϕ_2, ϕ_4) plane and the unit cell in this case is shown in Fig. 10b. Flow reversal at constant magnitude can be achieved from the phase change (0°, 180°). In the (ϕ_3, ϕ_4) plane the lattice vectors become (180°, 0°) and (90°, 180°) and a unit cell corresponding to these vectors is shown in Fig. 10(c). The simplest flow reversal vector in this plane is (90°, 0°).

Previously reported experimental data were collected in the (ϕ_2, ϕ_3) plane, which was perhaps not the best choice. The symmetry of these data reflect that of the torque functional, but both the shape of the maxima and their exact locations differ somewhat.

The 1:2:6 triad—This is the final example of a rational field for which we previously collected experimental data. Once again the torque functional demonstrates torque around the axis predicted by symmetry theory, which in this case is the odd axis. The computed magnitudes and the signs of the vorticity are in accord with the predictions of symmetry theory given in Table 2 of the ESI for Reference 11. In the (ϕ_1, ϕ_6) plane the lattice vectors are (0°, 360°) and (90°, 0°), which transform [S, S, S] to [S, S, S] and [C, S, S] respectively. Table 2 of the ESI for Reference 11 shows that symmetry theory predicts that the

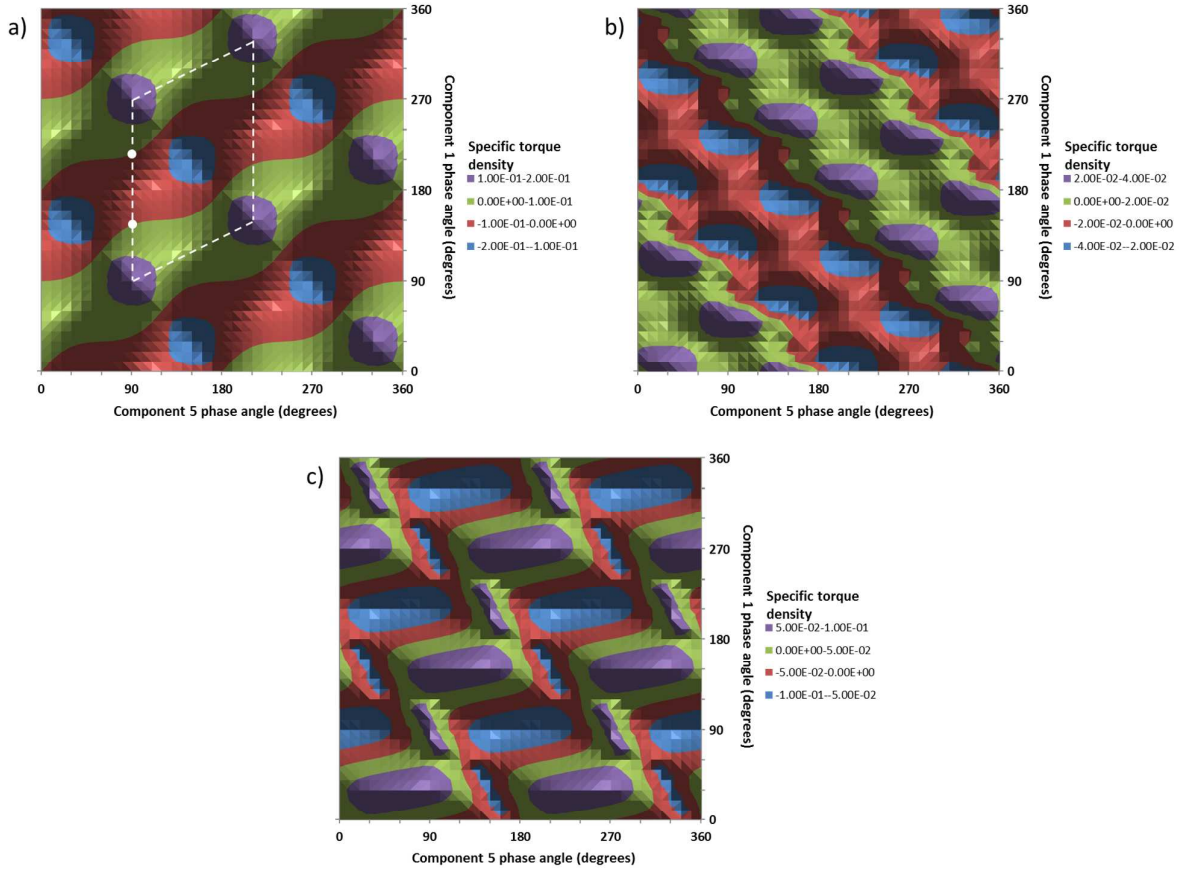

Fig. 12 The torque functional predicts torque around all axes for the 1:3:5 field: (a) around the *x* axis; (b) around the *y* axis; and (c) around the *z* axis.

torque density will be invariant for these fields. Flow reversal at constant magnitude can be achieved with the phase change (0°, 180°).

The equivalent phase angles are $(\phi_1,0,\phi_6), (\phi_1-\frac{1}{6}\phi_6,-\frac{1}{3}\phi_6,0), (0,-2\phi_1,\phi_6-6\phi_1)$. In the ($\phi_1$, ϕ_2) plane the lattice vectors transform to (60°, 120°) and (90°, 0°). In the (ϕ_2, ϕ_6) plane the lattice vectors become (0°, 360°) and (180°, 540°). The unit cells for each of these representations are evident in Fig. 11. Previously reported experimental data were taken in the (ϕ_1, ϕ_6) plane. These data reflect the symmetry of the torque functional, but the peak torques occur at somewhat different phase angles, demonstrating the limitations of the torque functional.

The 1:3:5 triad—Odd:odd:odd fields do not have the symmetry of vorticity and so we could not conclude anything about the torque created by these fields in our previous paper [11]. However, some interesting comments can be made about such fields. Recall that for symmetry-breaking, odd:odd fields the vorticity is invariant to the direction of the dc field. This fact implies that if the dc field is replaced by an alternating field fluid vorticity will still occur around the same axis. Indeed, odd:odd:dc and odd:odd:even both produce vorticity around the *z* axis. However, by the same logic odd:odd:odd fields should produce vorticity around all axes, so the situation is one of competing amplitudes, which is the domain of the torque functional.

For the 1:3:5 field the torque functional predicts torque around all field directions, so the net torque will be off axis. The computed torques around the *x*, *y*, and *z* axes are shown in Fig. 12. Under the qualitative reasoning of the previous paragraph torque around the *x* axis is produced by the 3,5 components. The torque functional peaks at 0.175 for this axis. The torque functional around the *z* axis peaks at 0.081 and can be roughly thought of as being created by the 1,3 components. Finally, the torque functional around the *y* axis peaks at only 0.0033 and can be approximately attributed to the 1,5 components. In fact, calculations for the balanced symmetry breaking field 1:3 produces a torque maximum of 0.163, for 3:5 the maximum is 0.067 and 1:5 maximizes at 0.002. The torque around the *y* axis is too small to measure, but the other torques were mapped out in the (ϕ_1, ϕ_5) plane, Fig. 13.

Although the experimental torque data almost appear sheared or skewed compared to those predicted by the functional in Fig. 12(a), both sets possess the same unit cell defined by the lattice vectors (180°, 0°) and (60°, 120°). Despite the fact that both sets of data possess the same *symmetry*, there is a phase shift between the predicted and experimental data indicated by the fact that the positions of the extrema are not in the exact same location in each phase map. The origin of this phase offset is not clear at this time, but was also seen with previously studied rational triads (*i.e.*, 1:2:3, 1:2:6, and 2:3:4) [11].

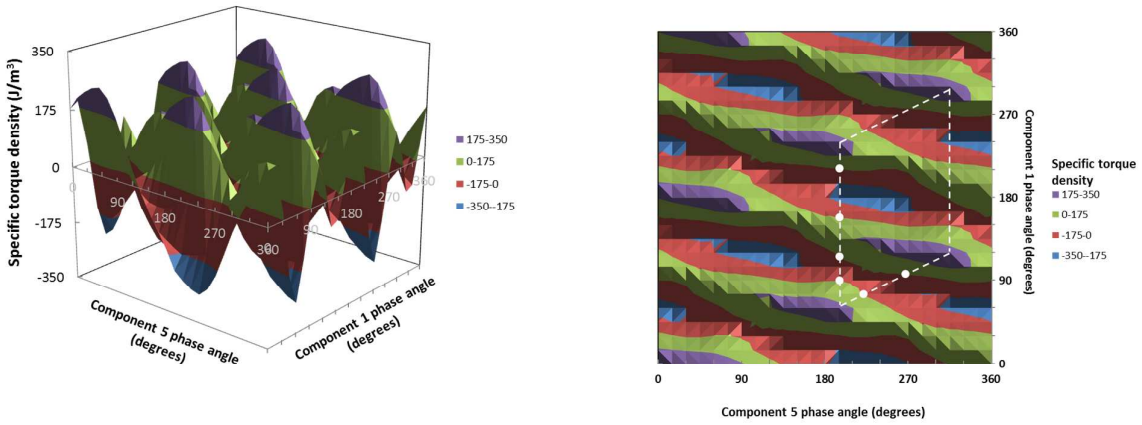

Fig. 13. Experimental torque density data for the (ϕ_1, ϕ_5) plane for a 1:3:5 rational triad (f_0=50Hz; B=150 Grms). These data possess the same unit cell and thus the same symmetry as those in Fig. 12(a) despite the superficial difference in their appearance.

There is a noteworthy consequence concerning *flow reversal* due to the subtle differences between the experimental data, which appear sheared, compared to those predicted by the functional. Recall that the locus of points that delineate the green and red regions in these torque density maps are points of *zero torque*, and thus indicate points of flow reversal. In both the predicted and experimental phase maps [Figs. 12(a) & 13], points of flow reversal are indicated by white dots on the boundary of the unit cell. The torque functional predicts no points of flow reversal on the canted boundaries and two points on the vertical boundaries; whereas, experiments reveal two points of flow reversal on the canted boundaries and four on the vertical boundaries.

4 Conclusions

We have developed a functional—by using physical insight and previous results based on the theory of vortex magnetic field mixing—that can be used to predict the relative *magnitude* and direction of the vorticity vector in magnetic particle suspensions driven by complex, time-dependent magnetic fields (symmetry-breaking rational fields and rational triads). We find that the functional predicts results that are in agreement with both the symmetry theories developed for these new classes of fields as well as experimental observations. Such a functional allows for the rapid investigation of innumerable magnetic field schemes, which can be used to direct future experimental work, and serves as a natural first step toward understanding the microscopic origins of the observed vorticity. Experimental results are given for a wide variety of symmetry-breaking fields, showing that the torque density falls off rapidly as the number of domains in the Lissajous plot increases. The 1:3:5 rational field was investigated experimentally and gives good agreement with the predictions of the torque functional. The vorticity direction produced by this field cannot be predicted by symmetry theory, but the torque density functional shows that the vorticity axis is not aligned with any of the three field components, and this is indeed the experimental observation.

Acknowledgements

Sandia National Laboratories is a multi-program laboratory managed and operated by Sandia Corporation, a wholly owned subsidiary of Lockheed Martin Corporation, for the U.S. Department of Energy's National Nuclear Security Administration under contract DE-AC04-94AL85000. This work was supported by the Laboratory-Directed Research and Development office at Sandia National Labs. We thank Matt Groo at Novamet for supplying the magnetic platelets.

References

1. S. Chandrasekhar, Hydrodynamic and Hydromagnetic Stability (Dover, New York, 1981), pp. 9–71.
2. A.V. Getling, Rayleigh-Bénard Convection: Structures and Dynamics (World Scientific, Singapore, 1997).
3. Dynamics of Spatio-Temporal Cellular Structures: Henri Bénard Centenary Review, edited by I. Mutabazi, J. E. Wesfreid, and E. Guyon (Springer, Berlin, 2005).
4. D.P. Lalas and S. Carmi, *Phys. Fluids*, 1971, **14**, 436.
5. R.A. Curtis, *Phys. Fluids*, 1971, **14**, 2096.
6. K.J. Solis and J.E. Martin, Isothermal magnetic advection: creating functional fluid flows for heat and mass transfer, *Appl. Phys. Lett.*, 2010, **97**, 034101.
7. J.E. Martin and K.J. Solis, Symmetry-breaking magnetic fields create a vortex fluid that exhibits a negative viscosity, active wetting, and strong mixing, *Soft Matter*, 2014, **10**, 3993–4002.
8. K.J. Solis and J.E. Martin, Torque density measurements on vortex fluids produced by symmetry-breaking rational magnetic fields, *Soft Matter*, 2014, **10**, 6139–6146.
9. K.J. Solis and J.E. Martin, Complex magnetic fields breathe life into fluids, *Soft Matter*, 2014, **10**, 9136–9142.
10. K.J. Solis and J.E. Martin, Multiaxial fields drive the thermal conductivity switching of a magneto-responsive platelet suspension, *Soft Matter*, 2013, **9**, 9182–9188.
11. J.E. Martin and K.J. Solis, Fully alternating, triaxial electric or magnetic fields offer new routes to fluid vorticity, *Soft Matter*, 2015, **11**, 241–254.

12. J.E. Martin, Theory of strong intrinsic mixing of particle suspensions in vortex magnetic fields, *Phys. Rev. E: Stat., Nonlinear, Soft Matter Phys.*, 2009, **79**, 011503.
13. J.E. Martin, A resonant biaxial Helmholtz coil employing a fractal capacitor bank, *Rev. Sci. Instrum.*, 2013, **84**, 094704.
14. J.E. Martin, R.A. Anderson, and C.P. Tigges, Simulation of the athermal coarsening of composites structured by a biaxial field, *J. Chem. Phys.*, 1998, 108, 7887.
15. J.E. Martin, E. Venturini, J. Odinek, and R.A. Anderson, Anisotropic magnetism in field-structured composites, *Phys. Rev. E*, 2000, **61**, 2818–2830.
16. J.E. Martin, R.A. Anderson, and R.L. Williamson, Generating strange magnetic and dielectric interactions: Classical molecules and particle foams, *J. Chem. Phys.*, 2003, **118**, 1557–1570.
17. M. E. Leunissen, H. R. Vutukuri, A. van Blaaderen, Directing colloidal self-assembly with biaxial electric fields, *Advanced Materials*, 2009, **21**, 3116.
18. B. Schwarzchild, Physics Nobel Prize Goes to Tsui, Stormer and Laughlin for the Fractional Quantum Hall Effect, *Physics Today*, December 1998.